Molecules and Cells

Mass Spectrometry-Based Screening Platform Reveals Orco Interactome in *Drosophila melanogaster*

Kate E. Yu[1,2], Do-Hyoung Kim[1,3], Yong-In Kim[2], Walton D. Jones[1,*], and J. Eugene Lee[2,*]

[1]Department of Biological Sciences, Korea Advanced Institute of Science and Technology, Daejeon 34141, Korea, [2]Center for Bioanalysis, Korea Research Institute of Standards and Science, Daejeon 34113, Korea, [3]Present address: School of Life Sciences, Gwangju Institute of Science and Technology, Gwangju 61005, Korea
*Correspondence: waltonjones@kaist.edu (WJ); j.eugenelee@gmail.com (JL)
http://dx.doi.org/10.14348/molcells.2018.2305
www.molcells.org

Animals use their odorant receptors to receive chemical information from the environment. Insect odorant receptors differ from the G protein-coupled odorant receptors in vertebrates and nematodes, and very little is known about their protein-protein interactions. Here, we introduce a mass spectrometric platform designed for the large-scale analysis of insect odorant receptor protein-protein interactions. Using this platform, we obtained the first Orco interactome from *Drosophila melanogaster*. From a total of 1,186 identified proteins, we narrowed the interaction candidates to 226, of which only two-thirds have been named. These candidates include the known olfactory proteins Or92a and Obp51a. Around 90% of the proteins having published names likely function inside the cell, and nearly half of these intracellular proteins are associated with the endomembrane system. In a basic loss-of-function electrophysiological screen, we found that the disruption of eight (i.e., Rab5, CG32795, Mpcp, Tom70, Vir-1, CG30427, Eaat1, and CG2781) of 28 randomly selected candidates affects olfactory responses *in vivo*. Thus, because this Orco interactome includes physiologically meaningful candidates, we anticipate that our platform will help guide further research on the molecular mechanisms of the insect odorant receptor family.

Keywords: *Drosophila*, odorant receptor, Orco, IP-MS, interactome

INTRODUCTION

In *Drosophila melanogaster*, odorant receptors (ORs) function on the dendritic membranes of olfactory sensory neurons (OSNs) (Clyne et al., 1999; Gao and Chess, 1999; Vosshall et al., 1999). OSNs reside in the third antennal segments and in the maxillary palps (Clyne et al., 1999; Gao and Chess, 1999; Vosshall et al., 1999) (Fig. 1A). These olfactory organs are covered with olfactory sensilla—porous needles that house the OSN dendrites floating in sensory lymph (Shanbhag et al., 2000). Most of these sensilla house two OSNs with each expressing one odor-specific OR in addition to the OR co-receptor Orco (Couto et al., 2005) (Fig. 1A). The activities of the different OSNs can be distinguished in single sensillum recordings (SSRs) by their characteristic amplitudes and sensitivity to different odorants (de Bruyne et al., 2001).

In contrast to the extensive neuron-level studies of peripheral olfactory systems using SSR, protein-level studies of insect ORs have lagged behind due to several factors. First, insect ORs are atypical among receptors with seven transmembrane domains. Insect ORs were initially expected to be G protein-coupled receptors (GPCRs) like the ORs in many other animals (Carlson, 1996), but their molecular characterization have been a considerable challenge because of insufficient sequence homology with other sensory chemoreceptor families (Bargmann, 2006; Clyne et al., 1999; Gao and

Received 17 November, 2017; revised 11 December, 2017; accepted 12 December, 2017; published online 12 February, 2018

eISSN: 0219-1032

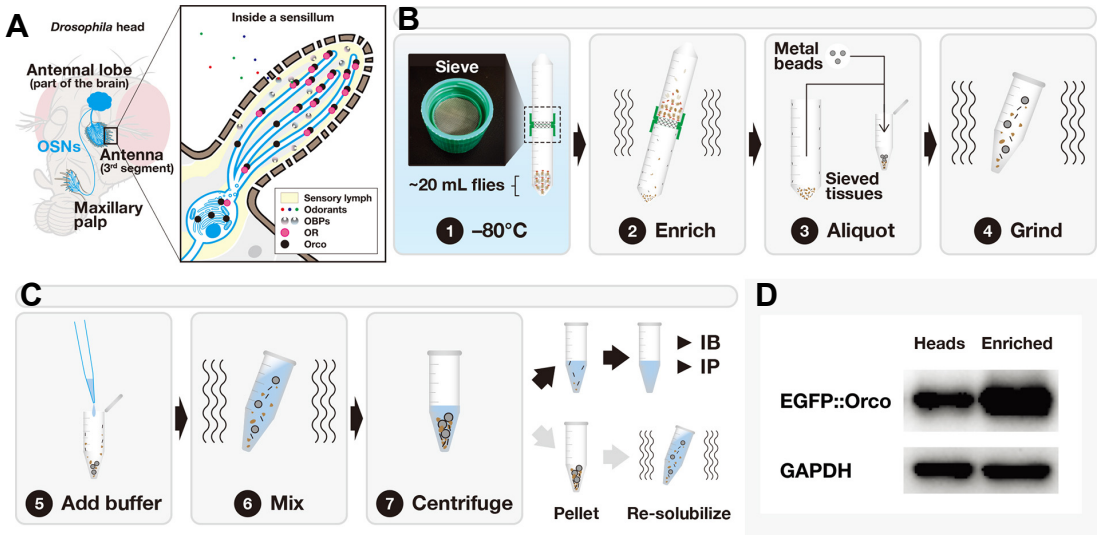

Fig. 1. Size-specific olfactory tissue enrichment accompanied with bead homogenization efficiently solubilizes Orco. (A) The anatomy of *Drosophila* OSNs and the functional locations of key olfactory proteins inside a sensillum. Elements are color coded. OSN, olfactory sensory neuron; OBP, odorant-binding protein; OR, odorant receptor. (B) The sieve filters larger body parts and enriches olfactory tissues. Sieved (enriched) tissues are vigorously shaken with metal beads to break open the exoskeleton. (C) Lysis buffer is added to the Ground (homogenized) tissues. A ready-to-use tissue lysate is obtained after two sequential rounds of centrifugation. Pellets can be analyzed to check the efficiency of protein solubilization (Supplementary Fig. S2). (D) Tissue enrichment by sieving concentrates Orco. A comparison is made with a head lysate. Antibodies are against EGFP and native GAPDH.

Chess, 1999; Vosshall et al., 1999), dependence on a co-receptor (Larsson et al., 2004), intracellular N-termini (Benton et al., 2006; Lundin et al., 2007; Smart et al., 2008; Tsitoura et al., 2010), ionotropic receptor-like properties (Sato et al., 2008; Wicher et al., 2008), putatively unique three-dimensional structures (Hopf et al., 2015), and discrete evolutionary lineage (Benton, 2015; Missbach et al., 2014; Nei et al., 2008). Second, insect ORs do not localize well to the plasma membrane in heterologous expression systems (Halty-deLeon et al., 2016), presumably because these systems inadequately mimic the native environment of insect OSNs. For this reason, heterologous systems are of limited value for discovering novel OR-interacting proteins. Third, not only do the OR proteins exist in small quantities because of their expression in so few cells (Vosshall et al., 1999), they are also physically sheltered inside tough and slender microstructures, the sensilla, *in vivo* (Shanbhag et al., 2000) (Fig. 1A). This makes it difficult to collect and manipulate the OR-containing tissues on a large scale. Thus, apart from homo- and heteromultimerization among themselves (Benton et al., 2006; Carraher et al., 2015; German et al., 2013; Nakagawa et al., 2012; Neuhaus et al., 2005), little is known about the proteins that physically associate with insect ORs.

As breakthroughs in our understanding of biological phenomena often come with methodological improvements, we wanted to establish a platform for the identification of unknown insect OR-related proteins. To do so, we chose to apply immunoprecipitation-mass spectrometry (IP-MS), a powerful method for discovering novel protein-protein interactions, to the identification of the first insect OR family interactome from Orco.

Orco is a fascinating member of the insect OR family. Unlike other ORs, Orco does not respond to natural odorants (Dobritsa et al., 2003; Elmore et al., 2003) and functions as a ubiquitous co-receptor for the other ORs (Larsson et al., 2004). Without Orco, the cellular localization of OR proteins is disrupted (Benton et al., 2006), preventing OSNs from responding to odors (Larsson et al., 2004). As Orco is expressed in nearly all OSNs (Larsson et al., 2004), the Orco interactome will likely provide insights into the general molecular mechanisms of insect olfaction.

Here, we report a platform that successfully identified candidate interaction partners of Orco from adult *Drosophila melanogaster*. To our knowledge, this is the first large-scale OR-related interactome obtained directly from insect olfactory tissues. The methods we have developed for olfactory tissue enrichment and Orco protein solubilization are coupled with IP-MS to provide a useful tool for exploring unknown protein-protein interactions. We analyzed the subcellular locations of the top 30% of the candidate interaction partners to probe the global trends of the co-immunoprecipitated proteins and validated that their loss-of-function alters olfactory physiology *in vivo*.

MATERIALS AND METHODS

Fly work

All EGFP-tagged Orco experiments were performed with *w*; Orco-GAL4, UAS-EGFP::Orco; *Orco*^{1} (Orco-GAL4 (Wang et al., 2003); UAS-EGFP::Orco (Benton et al., 2006); *Orco*^{1} (Larsson et al., 2004)). Background control experiments were performed with *w*; Orco-GAL4, UAS-myr::GFP; *Orco*^{1}

(myr::GFP (Pfeiffer et al., 2010)). The following UAS-RNAi flies were obtained from the Bloomington Drosophila Stock Center (Indiana, USA): Rab5 (#30518), Mpcp (#44508), Tom70 (#43966), vir-1 (#58209), CG30427 (#58271), Eaat1 (#43287), and CG2781 (#50710). All experimental flies were crossed to *w*; UAS-Dcr2; Orco-GAL4. GAL4 control flies were crossed either to attP40 (#36304) or attP2 (#36303) control lines. UAS control flies were crossed to w^{1118}. CG32795 was tested with a homozygous P element insertion mutant (#14771; Dmel\P{SUPor-P}CG32795[KG 08806]) whose heterozygous controls were in the w^{1118} background.

Tissue preparation

For the head lysate, 50 male and 50 female (total 100) heads with intact antennae, per tube, were manually dissected on dry ice. Flies for sieving were collected in 50-ml conical tubes up to 20 ml (including gaps) and kept at -80℃. The sieve (Fig. 1B) has a metal mesh (pore size 180 um^2) fixed in between two hollow lids. The assembled gadget was frozen at -80℃ for at least 30 min and then vigorously shaken on a vortexer. Per tube, 30 mg and 15 mg sieved tissues were used for IP and immunoblotting (IB), respectively. All tissues were homogenized at room temperature by three surgical stainless steel beads (3 mm in diameter) for 2 min with vigorous vortexing. Samples were kept on wet ice throughout the experiments if not being weighed or homogenized.

Total protein preparation

The lysates in Fig. 1D were prepared with the 2 × sodium dodecyl sulfate (SDS; Affymetrix/USB, J18220) buffer in the GFP-Trap®_A protocol (ver. 2014-12-18) offered by ChromoTek (Planegg-Martinsried, Germany). The rest of the lysates were prepared with 1% (v/v or w/v) of the indicated detergents in the dilution buffer for GFP-Trap®_A, with cOmplete™ EDTA-free Protease Inhibitor Cocktail (Roche, 04693159001) instead of the suggested protease inhibitors. The detergents used were Tween 20 (Biosesang, T1027), Triton X-100 (Bio Basic, TB0198), Nonidet P-40 (Bio Basic, NDB0385), Octyl-β-D-glucopyranoside (Fluka, 75083), n-Dodecyl β-D-maltoside (DDM; ThermoFisher, 89903), CHAPS (Sigma-Aldrich, C5070), CHAPSO (Calbiochem, 220201), and Zwittergent 3-16 (Calbiochem, 693023). 300 µl of lysis buffer was added per tube and the tube was vortexed for 1 min to produce a homogenous mixture. The mixture was then centrifuged for 5 min at 10,000 × g at 4℃ (10℃ for Zwittergent 3-16- or SDS-solubilized lysates) to remove tissue debris. The intermediate supernatant was transferred to a fresh tube and centrifuged once more to obtain the final transparent tissue lysate. Total protein quantification was performed with a Pierce™ BCA Protein Assay Kit (ThermoFisher, 23227). The final lysates were stored at -80℃.

Immunoblotting

Tissue lysates were mixed with the 2 × SDS buffer and heated at 50℃ for 30 min with 500-rpm vibration on an Eppendorf (Germany) ThermoMixer™ C. For the samples in Fig. 2B, equal volumes of a single lysate were aliquoted into six separate tubes and each tube was treated individually at 50, 55, 60, 65, and 70℃ for 30 min, and at 95℃ for 10 min. Other conditions were as described above. The samples were run on 10% SDS-PAGE and wet-transferred onto PVDF membranes (Merck, IPVH00010). Each well was loaded with 30 µg total protein. The membranes were incubated with primary antibodies overnight at 4℃. Anti-GFP (ThermoFisher, A-11122) diluted 1 to 5,000 in 5% skim milk/TBST was used to probe the GFP tags and anti- glyceraldehyde 3-phosphate dehydrogenase (GAPDH; abcam, ab125247) diluted 1 to 2,000 in TBST was used for the loading control. Secondary antibodies were incubated for 2 h at room temperature. HRP-conjugated antibodies against rabbit (Merck, AP132P) diluted 1 to 10,000 or mouse (ThermoFisher, 31430) diluted 1 to 5,000 were used. In all cases, the loading control was re-probed after stripping (Atto, WSE-7240).

Immunoprecipitation and on-bead digestion

All input materials for IP-MS were solubilized in fresh 1% (w/v) DDM lysis buffer made with MS-grade water. Per tube, 50 µl of GFP-Trap®_A bead slurry, equilibrated three times with 500 µl lysis buffer, and 5.0 mg total protein were added. Binding was conducted for 2 h on a rotating platform at room temperature. Harvested beads were washed five times with 1 ml lysis buffer and once with 1 ml Tris-HCl (pH 8.5). On-bead digestion was performed as previously described (Lee et al., 2011).

Mass spectrometric analysis

Following on-bead digestion, the tryptic peptides were desalted using StageTips packed with reversed-phase C18 material (3M, 2215) and dried using a vacuum concentrator. Dry samples were acidified by 0.1% formic acid for mass spectrometric analysis. Sample analyses were performed using an EASY-nLC 1000 (ThermoFisher) coupled to Q-Exactive mass spectrometer (ThermoFisher) equipped with a home-made nano-electrospray ion source. Peptides were separated on a 15-cm reversed phase column with 75-µm internal diameter packed in-house with 3-µm, 100-Å C18 beads (Agela Technologies) using a 130-min gradient from 9.5% to 36.5% acetonitrile in 0.1% formic acid at a flow rate of 350 nl/min. The mass spectrometer was operated in data-dependent mode to automatically switch between full-scan MS and tandem MS acquisition. Survey full scan mass spectra were acquired in an Orbitrap (300-1800 *m/z*) using automated gain control target of 1,000,000 ions and a resolution of 70,000. The top twelve most intense ions from the survey scan were isolated with automated gain control target of 500,000 ions at a resolution of 17,500. The isolated ions were fragmented in the high collision dissociation cell by collisionally-induced dissociation with 27% normalized collisional energy and 2 *m/z* isolation width.

Data analysis

The raw data files were searched using MaxQuant (version 1.6.0.1) (Cox and Mann, 2008) against the Uniprot *Drosophila melanogaster* database (UP000000803; Mar. 15, 2017). The search parameters were tryptic digestion, maximum of two missed cleavages, fixed carbamidomethyl mod-

ifications of cysteine, variable oxidation of methionine, and variable acetylation of protein N-termini. Mass tolerances for precursor ions were 4.5 ppm and those for fragment ions were 20 ppm. To determine the false discovery rate, a decoy database was constructed by reversing the target database. The protein and peptide level false discovery rates were fixed at 1% and we required that all proteins reported were identified by at least one unique peptide. Gene names were incorporated from the Database for Annotation, Visualization and Integrated Discovery (DAVID; v6.8) (Huang da et al., 2009). Gene Ontology annotations were obtained using Perseus (Tyanova et al., 2016) and additionally incorporated from UniProt (release 2017_07) and FlyBase (FB2017_03).

Single-sensillum recording

Flies were recorded on the 12th day after eclosion. SSRs from the A neurons of antennal basiconic 2 sensilla (ab2A; expressing Or59b) were obtained as previously described (Benton and Dahanukar, 2011). Methyl acetate (Sigma-Aldrich, 45999) was diluted 1 to 100,000 in paraffin oil (Sigma-Aldrich, 76235). Three sensilla each from a male and a female (total 6) were recorded first (Supplementary Fig. S6). If the initial recordings showed a phenotype, three additional sensilla each from a new male and a new female (for a total of 12) were recorded (Fig. 4). The statistical analyses and plotting were performed in PRISM (GraphPad Software, USA) using the two-way ANOVA with Bonferroni post-hoc tests for multiple comparisons. Statistical significance is indicated with asterisks ($*P \leq 0.05$, $**P \leq 0.01$, and $***P \leq 0.001$).

RESULTS

Tissue enrichment and protein solubilization

Because we sought to obtain the Orco interactome from adult olfactory tissues, we first set out to improve upon the existing tissue collection methods. To be efficient, we developed a custom sieve that enriches olfactory organs directly into a standard 50-ml conical tube (Fig. 1B). This arrangement allowed us to collect 10-20 ml of flies in a 50-mL conical tube and freeze them with the assembled sieve at -80℃. Then, upon vigorous shaking of the assembled gadget, all the smaller tissues break off from the fly bodies and fall into the opposite tube. Not only is our sieve method much faster and easier than manually collecting tissues (usually either antennae or heads), the sieved tissues also produced a better enrichment of EGFP-tagged Orco (Fig. 1D). Since our tissue collection method enriches Orco, we assumed it also enriches Orco-interacting proteins. We then achieved the most consistent outcome with metal bead-based homogenization (Supplementary Table S1). In this method, the sieved tissues and beads are shaken vigorously together in a microcentrifuge tube (Fig. 1B).

Because sieving breaks OSN axons, we solubilized total protein as quickly as possible (Fig. 1C). Unfortunately, despite numerous trials testing various conditions, none of the existing Orco-specific antibodies detected the native Orco protein on immunoblots (data not shown). For this reason, we decided to use an N-terminal EGFP-Orco fusion (EGFP::Orco) that was confirmed to be functional *in vivo* (Benton et al., 2006). We expressed EGFP::Orco in the Orco-null mutant (*Orco*^{1}) background to prevent the native Orco protein from competing for interaction partners. Next, we tested several laboratory detergents to optimize the solubilization of EGFP::Orco. We observed effective solubilization for all the tested detergents except Tween 20, CHAPS, and CHAPSO (Fig. 2A and Supplementary Fig. S2). We chose to use the mass spectrometry-compatible detergent DDM (previously shown to solubilize Orco from recombinant expression systems (Carraher et al., 2013)) at 1% (w/v) for the rest of the experiments. As we performed IB experiments, we noted that EGFP::Orco showed a curious temperature sensitivity during sample preparation, likely caused by its hydrophobicity. We were unable to reproduce DDM-solubilized EGFP::Orco immunoblots when the samples were heated to high temperatures in the presence of SDS and β-mercaptoethanol (Fig. 2B). To avoid this phenomenon, which is commonly observed in multi-pass membrane proteins (Okada et al., 2011), we optimized the conditions for working with EGFP::Orco. In the end, we achieved the most reproducible Orco immunoblots using a protocol that agitates the tissue lysates under mild heating to 50℃ (Fig. 2B).

Immunoprecipitation-mass spectrometry

To exclude any non-specific protein binding to the beads and to the bulky EGFP tag attached to Orco, we performed

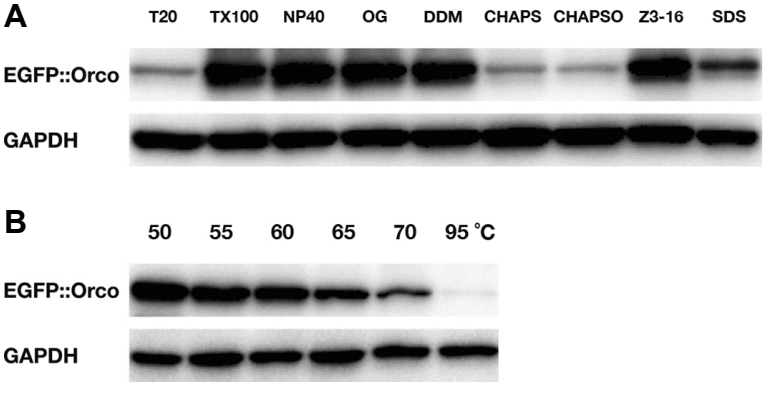

Fig. 2. Detergents and temperature affect Orco solubility. (A) Various laboratory detergents solubilizing Orco from enriched tissues. All detergents are at 1% (v/v or w/v). T20, Tween 20; TX100, Triton X-100; NP40, Nonidet P-40; OG, Octyl-β-D-glucopyranoside; DDM, n-Dodecyl β-D-maltoside; Z3-16, Zwittergent 3-16; SDS, sodium dodecyl sulfate. (B) Temperature sensitivity of Orco samples prepared from a 1% DDM lysate in the presence of SDS and β-mercaptoethanol. Antibodies are against EGFP and native GAPDH.

parallel IP experiments with a myristoylated GFP (myr::GFP). Note that the expression levels of EGFP::Orco and myr::GFP were not well-matched under our conditions (Supplementary Fig. S3). Although less than ideal, we used the myr::GFP-bound proteins as a background control because it was difficult to match the expression levels of the bait proteins *in vivo*. Finally, we performed the IP against the tags using an anti-GFP nanobody (the variable domain of the *Camelidae* heavy chain antibody (Harmsen and De Haard, 2007)) coupled to agarose beads.

We then performed liquid chromatography-tandem MS (LC-MS/MS) analyses to identify the co-immunoprecipitated proteins. Through trial and error, we discovered that on-bead tryptic digestion (Turriziani et al., 2014) most reproducibly reflects the bound proteins in the interactome. In this protocol, we added trypsin to the immunoprecipiated samples while they remained bound to the beads. The resulting tryptic peptides were then subjected to MS for protein identification.

Data processing and analyses

We searched the raw MS data against the UniProt *Drosophila melanogaster* database using MaxQuant. From the initial list of 1,186 identified proteins, we eliminated experimental group proteins without normalized peptide intensity (iBAQ) values in any of the technical replicates. Then, we ranked the remaining 753 proteins (Orco plus the 752 co-immunoprecipitated proteins) by their experimental-to-control iBAQ value ratios and decided to analyze an arbitrary portion—the top 227 proteins (top 30% of the 753 proteins)—as potential interactors (Fig. 3 and Supplementary Table S4). The resulting list contained Orco at the top followed by 144 proteins having no iBAQ values in the background control and 82 more proteins with high experimental-to-control iBAQ value ratios. The 144 proteins, designated Group A, are the primary Orco-interacting protein candidates (Table 1 and Supplementary Table S4). Group A included all the known olfactory proteins (i.e., Orco, Or92a, and Obp51a) identified in our data. The 82 proteins, designated Group B (Supplementary Table S4), generally had larger iBAQ values in the experimental samples than those in Group A. Note that there were numerous uncharacterized proteins without designated names (from the "CG genes") in both Group A and B (Supplementary Table S4). This result was unsurprising, as the percentage (32.2%) of these uncharacterized proteins closely matches the percentage (33.7%) of proteins without characterized functions in the soluble *Drosophila* antennal proteome (Anholt and Williams, 2010).

Next, we performed an automatic Gene Ontology search for the 227 proteins (Orco plus the 226 interaction candidates) (Supplementary Table S4). Although the search assigned predicted features to the uncharacterized proteins, we only analyzed proteins with published names to improve accuracy (Fig. 3). For 154 (67.8% of the 227 proteins) proteins, these search results were manually curated for subcellular locations (Cellular Component Ontology) (Fig. 3 and Supplementary Table S4) to identify any global trends among the Orco-interacting candidates under our conditions. Note that in the tallies, individual proteins may be counted more than once if they are found at multiple subcellular locations. In addition, we performed an Ingenuity® Pathway Analysis with these 227 proteins to identify networks or pathways associated with the Orco interactome (Supplementary Fig. S5). Although the search results were heavily biased toward mammalian systems, they were suggestive of cellular activities related to membrane proteins.

Physiological validation of the interactome

Using orthogonal methods, we sought to validate whether these 226 proteins are biologically relevant Orco-interacting partners. We decided to determine if any of the proteins affect the odor-evoked responses of OSNs, which we took as an indication of OR-Orco protein complex functionality. We

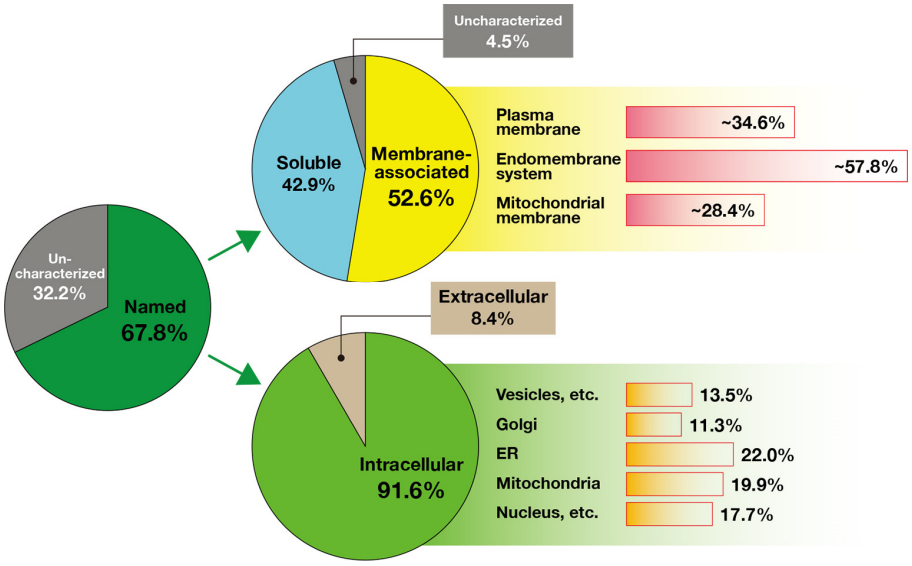

Fig. 3. Subcellular locations of the select Orco-interacting candidates. The analysis of the top 227 proteins. Cellular Component Ontology was automatically retrieved by Perseus and additional information was incorporated from UniProt and FlyBase. Single proteins may be counted in multiple categories. Refer to Supplementary Table S4 for details.

Table 1. The top 20 Orco-interacting candidates and their representative Gene Ontology annotations. Gene Ontology annotations were retrieved using Perseus (Tyanova et al., 2016). Refer to Supplementary Table S5 for details.

Rank	Gene name	iBAQ value	PSM	Representative cellular component ontology (by Perseus)	Representative molecular function ontology (by Perseus)
1	Orco	1.01×10^9	434	Dendrite, integral to membrane, plasma membrane	Calcium channel activity, calmodulin binding, ligand-gated ion channel activity, olfactory receptor activity, passive transmembrane transporter activity, protein dimerization activity
2	CG4962	1.69×10^8	4	(None)	(None)
3	Tspo	1.44×10^8	13	Integral to membrane, mitochondrial outer membrane	(None)
4	Rac1	5.94×10^7	14	Cytosol, extrinsic to plasma membrane, intracellular, plasma membrane, rhabdomere	GTPase activity
5	SsRbeta	5.90×10^7	13	Endomembrane system, integral to membrane, microtubule associated complex, ribonucleoprotein complex, signal recognition particle (endoplasmic reticulum targeting)	Peptide binding, signal sequence binding
6	Acp53C14a	5.43×10^7	9	Extracellular space	(None)
7	MSBP	4.91×10^7	15	Endomembrane system, plasma membrane	Cation binding, ecdysone binding, heme binding
8	Sfp26Ad	3.58×10^7	7	Extracellular space	(None)
9	Rab5	3.43×10^7	15	Early endosome, membrane-bounded vesicle, neuronal cell body, plasma membrane, synapse	GTPase activity
10	CG9034	3.42×10^7	7	(None)	(None)
11	CdsA	3.15×10^7	16	Endoplasmic reticulum membrane, integral to membrane, plasma membrane	Cytidylyltransferase activity, transferase activity transferring phosphorus-containing groups
12	Arf79F	2.83×10^7	8	Golgi stack, intracellular	GTPase activity
13	sea	2.22×10^7	24	Integral to membrane, mitochondrion, Nebenkern	(None)
14	mub	2.18×10^7	9	Nucleus	RNA binding
15	CG14407	2.18×10^7	6	(None)	Electron carrier activity, oxidoreductase activity acting on a sulfur group of donors
16	CG15386	2.06×10^7	6	(None)	(None)
17	CG16758	2.04×10^7	12	Cytoplasm	Purine-nucleoside phosphorylase activity, transferase activity transferring glycosyl/pentosyl groups
18	CG5676	2.00×10^7	7	(None)	(None)
19	ND5	1.94×10^7	8	Integral to membrane, mitochondrial inner membrane, respiratory chain	NADH dehydrogenase activity
20	CG6178	1.94×10^7	16	Microbody, peroxisome	Long-chain fatty acid-CoA ligase activity
21	CG34309	1.85×10^7	3	(None)	(None)

PSM, Peptide spectrum matches

randomly selected 28 proteins, used either RNAi knockdowns or P element insertion mutants in live animals, and recorded odor-evoked OSN activities with SSR. Since any defects in Orco-related functionality would likely affect all ORs, our priority was choosing an OSN subclass that would most clearly show the contrast between the wild-type flies

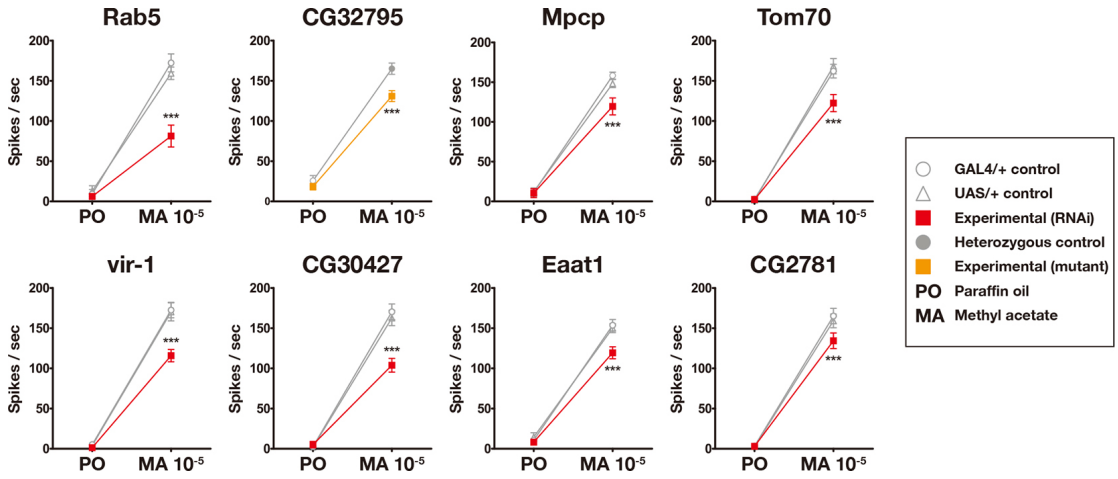

Fig. 4. The Orco-interacting candidates affect odor-evoked OSN activities *in vivo*. Details about the symbols and abbreviations are shown in the box. Rab5 (monomeric GTPase); CG32795, TMPIT-like protein (InterPro suggestion); Mpcp, Mitochondrial phosphate carrier protein; Tom70, Translocase of outer membrane 70; vir-1, virus-induced RNA 1; CG30427, Fatty acyl-CoA reductase (UniProt recommendation); Eaat1, Excitatory amino acid transporter 1; CG2781, Elongation of very long chain fatty acids protein (UniProt recommendation). Statistical significance was determined using two-way ANOVA with Bonferroni post-hoc tests for multiple comparisons. $*P \leq 0.05$, $**P \leq 0.01$, and $***P \leq 0.001$.

and those with loss-of-function in the candidate Orco-interacting proteins. For such purpose, we chose to record from the A neurons of the antennal basiconic 2 sensilla (ab2A; expressing Or59b) using methyl acetate (MA) as a stimulus. While none of the disrupted candidates increased ab2A responses to MA, eight showed significantly decreased activities (Fig. 4) and 20 showed no change (Supplementary Fig. S6). Thus, because multiple candidates are associated with the odor-evoked activities of OSNs, we consider our interaction candidate list a valuable resource for future applications and studies in insect olfaction.

DISCUSSION

Despite the significance of their molecular features, few studies have been able to directly address the cellular machineries by which the insect ORs associate in the neurons. Our goal, therefore, was to obtain insect OR interactomes composed of native OSN proteins harvested from their original tissue environments to discover their protein-protein interactions. To this end, we obtained proteins from enriched olfactory tissues that were co-immunoprecipitated with the universal insect OR co-receptor Orco.

Tissue manipulation protocols were critical because we wanted our results to reflect the native OSN proteome. The extraction and isolation of OR proteins from adult olfactory organs in *Drosophila* is difficult because the olfactory neurons are enclosed in exoskeletal microstructures. The soluble proteome of the antenna has been reported (Anholt and Williams, 2010), but membrane proteins are more difficult to solubilize from tissues. An ionotropic receptor (IR) protein complex was isolated from antennae (Ai et al., 2013), but because the ORs are thought to be more hydrophobic (ORs have more putative transmembrane domains than IRs) and possibly form heteromultimers, further optimization of the extraction conditions was necessary. In addition, we wanted to extract Orco with intact protein complexes to analyze its interactome. Eventually, we were able to optimize the conditions and overcome these challenges (Fig. 1 and Fig. 2). Since we used enriched adult olfactory tissues, proteins native to insect OSNs were included as prey proteins for the IP. This is something heterologous expression systems cannot replicate. However, because our antibodies for native Orco do not work with the IB or IP techniques, we were forced to use the GAL4-UAS over-expression system to express a tagged version of Orco in Orco-positive neurons. Because bait protein over-expression represents a deviation from the wild-type cellular environment, it can lead to an increase in the identification of non-specific interactions. Still, the EGFP tag does not dramatically alter the olfactory function or subcellular localization of EGFP::Orco *in vivo* (Benton et al., 2006), suggesting regular functionality and regular interactions.

The proteins we identified manifest both intra- and extracellular interactions, suggesting our platform is appropriate for broad-range screening. Yet, in our particular sample preparation conditions involving aggressive tissue manipulation, a high detergent concentration, and room-temperature IP, it is likely that strong interactions remained and interactions with abundant proteins were readily restored, but weak interactions, conditional interactions, or trace effectors may have been lost (Gingras et al., 2007). Furthermore, proteins that bind the Orco N-terminus may be underrepresented because of steric hindrance by the EFGP tag. One expected Orco-interacting protein, calmodulin (Bahk and Jones, 2016), did not appear in our data, perhaps reflecting the conditional nature of its interaction with Orco (Bahk and Jones, 2016; Mukunda et al., 2016). Nor did another likely

Orco interaction partner, dATP8B (Ha et al., 2014; Liu et al., 2014), appear in our data. Although SNMP is reportedly associated with either the Or67d-Orco protein complex in pheromone-sensing OSNs (Benton et al., 2007; Jin et al., 2008; Li et al., 2014) or the Or22a-Orco protein complex in an insect cell line (German et al., 2013), we were unable to identify the protein in our IP-MS dataset. This result was probably a consequence of being unable to co-immunoprecipitate Or67d or Or22a with Orco. For the same reason, we were unsuccessful in detecting the Or67d-associating LUSH (Obp76a) (Laughlin et al., 2008). Instead of LUSH, however, we found Obp51a among the top-ranking Orco interaction candidates (the Group A proteins). The odorant-binding proteins (OBPs) are predicted to mainly release odorants near ORs rather than bind to ORs directly (Leal, 2013; Venthur et al., 2014), but as the pheromone-binding LUSH most likely interacts with Or67d (Laughlin et al., 2008), our identification of Obp51a implies the existence of alternative mechanisms for OBP-OR-Orco interactions.

Even with the awareness of the subtle nature of interactions, we were surprised to identify only one (Or92a) of the 43 ORs expressed in adult olfactory tissues (Couto et al., 2005) (Supplementary Table S4). There is abundant evidence that Orco heteromultimerizes with other members of the insect OR family (Benton et al., 2006; Carraher et al., 2015; German et al., 2013; Nakagawa et al., 2012; Neuhaus et al., 2005); thus, we expected to find many more ORs appearing in the Orco interactome. The lack of ORs may be a consequence of their generally low expression levels, which arise mainly from the small number of olfactory neurons. It is worth mentioning that one of the techniques used to discover the insect ORs was screening for mRNAs with extremely low expression levels in the olfactory organs (Vosshall et al., 1999). Consistent with our data, a study of the antennal proteome of *Bombyx mori* (silkmoth) found only one OR of its 30 adult ORs (Tanaka et al., 2009) among a total of 364 proteins (Zhao et al., 2015). Meanwhile, our identification of Or92a is not particularly odd because it is expressed at relatively higher expression levels in more cells in the antenna than the other ORs (Couto et al., 2005; Fishilevich and Vosshall, 2005; Jafari et al., 2012). We expect sieving the tissues with a finer mesh and conducting IP at lower temperatures may improve this result in future experiments.

Considering the typical subcellular location of Orco (i.e., in the dendrites and soma) and considering its overexpression in the tissues used in this study, it is unsurprising that we identified many ER-related proteins (22% of the annotated intracellular proteins). Our unexpected identification of so many mitochondrial proteins (~20% of the annotated intracellular proteins) may simply reflect the abundance of mitochondria in olfactory dendrites. But if any of these proteins turn out to be true Orco interactors, their presence in our list may indicate a novel aspect of Orco protein physiology. One possible explanation is that the OR-Orco protein complex and mitochondria share the dendritic trafficking machinery (Schwarz, 2013). The relationship between Orco, these mitochondrial proteins, and dendritic trafficking can be examined to clarify their roles. We would also like to suggest that mitochondria-associated ER membranes (MAMs) (Rowland and Voeltz, 2012) may play a role in Orco's function. MAMs designate the regions where ER membranes and mitochondria physically associate. MAMs are known to regulate lipid synthesis and intracellular calcium signaling, where most importantly, the roles of mitochondria in the calcium-mediated responses of mouse OSNs have been described (Fluegge et al., 2012). If Orco plays a role in such coordination systems, many fascinating discoveries in the field of insect olfaction lie ahead.

We found reduced odor-evoked responses in OSNs in which one of the eight proteins (i.e., Rab5, CG32795, Mpcp, Tom70, vir-1, CG30427, Eaat1, and CG2781) was depleted. Ideally, these reduced responses reflect functional disruption of Orco-interacting proteins. This result must be cautiously interpreted, however, because electrophysiological responses are sophisticated cellular phenomena. Although it is reasonable to expect the depletion of Orco-interacting candidates to affect odor-evoked OSN responses by disturbing proper Orco function, the down-regulation of false positive proteins that are independently involved in cell maintenance or action potential generation may produce false positive electrophysiological results. More functional studies are required to clarify the biological meanings of our SSR results.

Together, the significance of our results rests on the fact that all of the candidate interaction partners we discovered through this platform originated in the native tissue environment of the bait protein. The identified proteins provide a new perspective on the protein-protein interactions of Orco. Our results are also important because our technique represents a methodological advance. Other OR interactomes can be similarly examined using our protocol, even those of other insect species. We anticipate our platform will facilitate further studies on the molecular mechanisms of insect ORs and will prove versatile in other insect tissue-based interactome analyses.

Note: Supplementary information is available on the Molecules and Cells website (www.molcells.org).

ACKNOWLEDGMENTS

We thank Sion Lee for donating *w;* Orco-GAL4, UAS-EGFP::Orco; *Orco*^{1} and Sujin Yu for assisting with editing the figures. We also thank Kyung-Ok Cho and Woo Rin Lee for helpful comments on the manuscript. Fly stocks obtained from the Bloomington Drosophila Stock Center (NIH P40OD018537) were used in this study. This research was supported by grant DRC-14-2-KRISS awarded to J.E.L. from National Research Council of Science and Technology.

REFERENCES

Ai, M., Blais, S., Park, J.Y., Min, S., Neubert, T.A., and Suh, G.S. (2013). Ionotropic glutamate receptors IR64a and IR8a form a functional odorant receptor complex *in vivo* in *Drosophila*. J. Neurosci. *33*, 10741-10749.

Anholt, R.R., and Williams, T.I. (2010). The soluble proteome of the Drosophila antenna. Chem. Senses *35*, 21-30.

Bahk, S., and Jones, W.D. (2016). Insect odorant receptor trafficking

requires calmodulin. BMC Biol. *14*, 83.

Bargmann, C.I. (2006). Comparative chemosensation from receptors to ecology. Nature *444*, 295-301.

Benton, R. (2015). Multigene family evolution: perspectives from insect chemoreceptors. Trends Ecol. Evol. *30*, 590-600.

Benton, R., and Dahanukar, A. (2011). Electrophysiological recording from Drosophila olfactory sensilla. Cold Spring Harb. Protoc. *2011*, 824-838.

Benton, R., Sachse, S., Michnick, S.W., and Vosshall, L.B. (2006). Atypical membrane topology and heteromeric function of Drosophila odorant receptors *in vivo*. PLoS Biol *4*, e20.

Benton, R., Vannice, K.S., and Vosshall, L.B. (2007). An essential role for a CD36-related receptor in pheromone detection in Drosophila. Nature *450*, 289-293.

Carlson, J.R. (1996). Olfaction in Drosophila: from odor to behavior. Trends Genet. *12*, 175-180.

Carraher, C., Nazmi, A.R., Newcomb, R.D., and Kralicek, A. (2013). Recombinant expression, detergent solubilisation and purification of insect odorant receptor subunits. Protein Expr. Purif. *90*, 160-169.

Carraher, C., Dalziel, J., Jordan, M.D., Christie, D.L., Newcomb, R.D., and Kralicek, A.V. (2015). Towards an understanding of the structural basis for insect olfaction by odorant receptors. Insect Biochem. Mol. Biol. *66*, 31-41.

Clyne, P.J., Warr, C.G., Freeman, M.R., Lessing, D., Kim, J., and Carlson, J.R. (1999). A novel family of divergent seven-transmembrane proteins: candidate odorant receptors in Drosophila. Neuron *22*, 327-338.

Couto, A., Alenius, M., and Dickson, B.J. (2005). Molecular, anatomical, and functional organization of the Drosophila olfactory system. Curr. Biol. *15*, 1535-1547.

Cox, J., and Mann, M. (2008). MaxQuant enables high peptide identification rates, individualized p.p.b.-range mass accuracies and proteome-wide protein quantification. Nat. Biotechnol. *26*, 1367-1372.

de Bruyne, M., Foster, K., and Carlson, J.R. (2001). Odor coding in the Drosophila antenna. Neuron *30*, 537-552.

Dobritsa, A.A., van der Goes van Naters, W., Warr, C.G., Steinbrecht, R.A., and Carlson, J.R. (2003). Integrating the molecular and cellular basis of odor coding in the Drosophila antenna. Neuron *37*, 827-841.

Elmore, T., Ignell, R., Carlson, J.R., and Smith, D.P. (2003). Targeted mutation of a Drosophila odor receptor defines receptor requirement in a novel class of sensillum. J. Neurosci. *23*, 9906-9912.

Fishilevich, E., and Vosshall, L.B. (2005). Genetic and functional subdivision of the Drosophila antennal lobe. Curr. Biol. *15*, 1548-1553.

Fluegge, D., Moeller, L.M., Cichy, A., Gorin, M., Weth, A., Veitinger, S., Cainarca, S., Lohmer, S., Corazza, S., Neuhaus, E.M., et al. (2012). Mitochondrial Ca(2+) mobilization is a key element in olfactory signaling. Nat. Neurosci. *15*, 754-762.

Gao, Q., and Chess, A. (1999). Identification of candidate Drosophila olfactory receptors from genomic DNA sequence. Genomics *60*, 31-39.

German, P.F., van der Poel, S., Carraher, C., Kralicek, A.V., and Newcomb, R.D. (2013). Insights into subunit interactions within the insect olfactory receptor complex using FRET. Insect Biochem. Mol. Biol. *43*, 138-145.

Gingras, A.C., Gstaiger, M., Raught, B., and Aebersold, R. (2007). Analysis of protein complexes using mass spectrometry. Nat. Rev. Mol. Cell Biol. *8*, 645-654.

Ha, T.S., Xia, R., Zhang, H., Jin, X., and Smith, D.P. (2014). Lipid flippase modulates olfactory receptor expression and odorant sensitivity in Drosophila. Proc. Natl. Acad. Sci. USA *111*, 7831-7836.

Halty-deLeon, L., Miazzi, F., Kaltofen, S., Hansson, B.S., and Wicher, D. (2016). The mouse receptor transporting protein RTP1S and the fly SNMP1 support the functional expression of the Drosophila odorant coreceptor Orco in mammalian culture cells. J. Neurosci. Methods *271*, 149-153.

Harmsen, M.M., and De Haard, H.J. (2007). Properties, production, and applications of camelid single-domain antibody fragments. Appl. Microbiol. Biotechnol. *77*, 13-22.

Hopf, T.A., Morinaga, S., Ihara, S., Touhara, K., Marks, D.S., and Benton, R. (2015). Amino acid coevolution reveals three-dimensional structure and functional domains of insect odorant receptors. Nat. Commun. *6*, 6077.

Huang, D.W., Sherman, B.T., and Lempicki, R.A. (2009). Systematic and integrative analysis of large gene lists using DAVID bioinformatics resources. Nat. Protoc. *4*, 44-57.

Jafari, S., Alkhori, L., Schleiffer, A., Brochtrup, A., Hummel, T., and Alenius, M. (2012). Combinatorial activation and repression by seven transcription factors specify Drosophila odorant receptor expression. PLoS Biol. *10*, e1001280.

Jin, X., Ha, T.S., and Smith, D.P. (2008). SNMP is a signaling component required for pheromone sensitivity in Drosophila. Proc. Natl. Acad. Sci. USA *105*, 10996-11001.

Larsson, M.C., Domingos, A.I., Jones, W.D., Chiappe, M.E., Amrein, H., and Vosshall, L.B. (2004). Or83b encodes a broadly expressed odorant receptor essential for Drosophila olfaction. Neuron *43*, 703-714.

Laughlin, J.D., Ha, T.S., Jones, D.N.M., and Smith, D.P. (2008). Activation of pheromone-sensitive neurons is mediated by conformational activation of pheromone-binding protein. Cell *133*, 1255-1265.

Leal, W.S. (2013). Odorant reception in insects: roles of receptors, binding proteins, and degrading enzymes. Annu. Rev. Entomol. *58*, 373-391.

Lee, J.E., Sweredoski, M.J., Graham, R.L., Kolawa, N.J., Smith, G.T., Hess, S., and Deshaies, R.J. (2011). The steady-state repertoire of human SCF ubiquitin ligase complexes does not require ongoing Nedd8 conjugation. Mol. Cell Proteomics *10*, M110 006460.

Li, Z., Ni, J.D., Huang, J., and Montell, C. (2014). Requirement for Drosophila SNMP1 for rapid activation and termination of pheromone-induced activity. PLoS Genet. *10*, e1004600.

Liu, Y.C., Pearce, M.W., Honda, T., Johnson, T.K., Charlu, S., Sharma, K.R., Imad, M., Burke, R.E., Zinsmaier, K.E., Ray, A., et al. (2014). The *Drosophila melanogaster* phospholipid flippase dATP8B is required for odorant receptor function. PLoS Genet. *10*, e1004209.

Lundin, C., Kall, L., Kreher, S.A., Kapp, K., Sonnhammer, E.L., Carlson, J.R., Heijne, G., and Nilsson, I. (2007). Membrane topology of the Drosophila OR83b odorant receptor. FEBS Lett. *581*, 5601-5604.

Missbach, C., Dweck, H.K., Vogel, H., Vilcinskas, A., Stensmyr, M.C., Hansson, B.S., and Grosse-Wilde, E. (2014). Evolution of insect olfactory receptors. Elife *3*, e02115.

Mukunda, L., Miazzi, F., Sargsyan, V., Hansson, B.S., and Wicher, D. (2016). Calmodulin Affects Sensitization of *Drosophila melanogaster* Odorant Receptors. Front. Cell Neurosci. *10*, 28.

Nakagawa, T., Pellegrino, M., Sato, K., Vosshall, L.B., and Touhara, K. (2012). Amino acid residues contributing to function of the heteromeric insect olfactory receptor complex. PLoS One *7*, e32372.

Nei, M., Niimura, Y., and Nozawa, M. (2008). The evolution of animal chemosensory receptor gene repertoires: roles of chance and necessity. Nat. Rev. Genet. *9*, 951-963.

Neuhaus, E.M., Gisselmann, G., Zhang, W., Dooley, R., Stortkuhl, K., and Hatt, H. (2005). Odorant receptor heterodimerization in the olfactory system of *Drosophila melanogaster*. Nat. Neurosci. *8*, 15-17.

Okada, N., Yamamoto, T., Watanabe, M., Yoshimura, Y., Obana, E., Yamazaki, N., Kawazoe, K., Shinohara, Y., and Minakuchi, K. (2011). Identification of TMEM45B as a protein clearly showing thermal aggregation in SDS-PAGE gels and dissection of its amino acid sequence responsible for this aggregation. Protein Expr. Purif *77*, 118-123.

Pfeiffer, B.D., Ngo, T.T., Hibbard, K.L., Murphy, C., Jenett, A., Truman, J.W., and Rubin, G.M. (2010). Refinement of tools for targeted gene expression in Drosophila. Genetics *186*, 735-755.

Rowland, A.A., and Voeltz, G.K. (2012). Endoplasmic reticulum-mitochondria contacts: function of the junction. Nat. Rev. Mol. Cell Biol. *13*, 607-625.

Sato, K., Pellegrino, M., Nakagawa, T., Nakagawa, T., Vosshall, L.B., and Touhara, K. (2008). Insect olfactory receptors are heteromeric ligand-gated ion channels. Nature *452*, 1002-1006.

Schwarz, T.L. (2013). Mitochondrial trafficking in neurons. Cold Spring Harb. Perspect Biol. *5*.

Shanbhag, S.R., Muller, B., and Steinbrecht, R.A. (2000). Atlas of olfactory organs of *Drosophila melanogaster* 2. Internal organization and cellular architecture of olfactory sensilla. Arthropod. Struct. Dev. *29*, 211-229.

Smart, R., Kiely, A., Beale, M., Vargas, E., Carraher, C., Kralicek, A.V., Christie, D.L., Chen, C., Newcomb, R.D., and Warr, C.G. (2008). Drosophila odorant receptors are novel seven transmembrane domain proteins that can signal independently of heterotrimeric G proteins. Insect Biochem. Mol. Biol. *38*, 770-780.

Tanaka, K., Uda, Y., Ono, Y., Nakagawa, T., Suwa, M., Yamaoka, R., and Touhara, K. (2009). Highly selective tuning of a silkworm olfactory receptor to a key mulberry leaf volatile. Curr. Biol. *19*, 881-890.

Tsitoura, P., Andronopoulou, E., Tsikou, D., Agalou, A., Papakonstantinou, M.P., Kotzia, G.A., Labropoulou, V., Swevers, L., Georgoussi, Z., and Iatrou, K. (2010). Expression and membrane topology of Anopheles gambiae odorant receptors in lepidopteran insect cells. PLoS One *5*, e15428.

Turriziani, B., Garcia-Munoz, A., Pilkington, R., Raso, C., Kolch, W., and von Kriegsheim, A. (2014). On-beads digestion in conjunction with data-dependent mass spectrometry: a shortcut to quantitative and dynamic interaction proteomics. Biology (Basel) *3*, 320-332.

Tyanova, S., Temu, T., Sinitcyn, P., Carlson, A., Hein, M.Y., Geiger, T., Mann, M., and Cox, J. (2016). The Perseus computational platform for comprehensive analysis of (prote)omics data. Nat. Methods *13*, 731-740.

Venthur, H., Mutis, A., Zhou, J.-J., and Quiroz, A. (2014). Ligand binding and homology modelling of insect odorant-binding proteins. Physiol. Entomol. *39*, 183-198.

Vosshall, L.B., Amrein, H., Morozov, P.S., Rzhetsky, A., and Axel, R. (1999). A spatial map of olfactory receptor expression in the Drosophila antenna. Cell *96*, 725-736.

Wang, J.W., Wong, A.M., Flores, J., Vosshall, L.B., and Axel, R. (2003). Two-photon calcium imaging reveals an odor-evoked map of activity in the fly brain. Cell *112*, 271-282.

Wicher, D., Schafer, R., Bauernfeind, R., Stensmyr, M.C., Heller, R., Heinemann, S.H., and Hansson, B.S. (2008). Drosophila odorant receptors are both ligand-gated and cyclic-nucleotide-activated cation channels. Nature *452*, 1007-1011.

Zhao, Y., Li, H., and Miao, X. (2015). Proteomic analysis of silkworm antennae. J. Chem. Ecol. *41*, 1037-1042.